Aquaculture 623 (2026) 744129

Contents lists available at ScienceDirect

Aquaculture

journal homepage: www.elsevier.com/locate/aquaculture

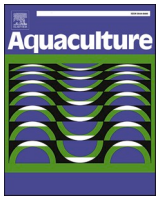

Red-spotted Grouper Nervous Necrosis Virus (RGNNV) detection in giant grouper (*Epinephelus lanceolatus*) using destructive and non-destructive samples is influenced by infectious dose, challenge route, and infection outcome

Ngoc-Tran T. Nguyen [a,b,*], Junya Minami [a,b], Maria Andrade Martinez [a,c], Richard M. Knuckey [b,d], Kyall R. Zenger [a,b], Dean R. Jerry [a,b,c,e], Kelly Condon [a,b,c,*]

[a] College of Science and Engineering, James Cook University, Townsville, QLD 4814, Australia
[b] Australian Research Council Industrial Transformation Research Hub (ARC ITRH) for Supercharging Tropical Aquaculture through Genetic Solutions, James Cook University, Townsville, QLD 4814, Australia
[c] JCU AquaPATH Lab, James Cook University, Townsville, QLD 4814, Australia
[d] The Company ONE, 9-15 Aumuller Street, Cairns, QLD 4870, Australia
[e] Tropical Futures Institute, James Cook University, Singapore

ARTICLE INFO

Keywords:
Red-spotted grouper nervous necrosis virus
Giant grouper
Destructive
Non-destructive
Mucous

ABSTRACT

Viral Encephalopathy and Retinopathy (VER), caused by Red-spotted Grouper Nervous Necrosis Virus (RGNNV), is a major constraint on giant grouper (*Epinephelus lanceolatus*) aquaculture. Current surveillance depends on destructive brain and eye sampling, limiting scalable and repeated monitoring of broodstock and high-value fish. This study evaluated detection performance of destructive and non-destructive sampling methods for RGNNV in giant grouper following experimental intramuscular injection challenge. One hundred juvenile giant groupers were challenged with four RGNNV doses (4.6×10^7, 4.6×10^6, 4.6×10^5 and 4.6×10^4 copies/mL) in duplicate tanks, each containing five cages (10 fish/cage) representing four dose groups and one cohabitated control. RGNNV copy number was quantified by RT-qPCR across nine destructive tissues (brain, eyes, nostril, gill, head kidney, spleen, injection-site muscle and gut), two non-destructive samples (mucous and urine), and parallel tank water environmental RNA (eRNA). Fish morbidity increased dose-dependently, from 30% at 4.6×10^4 to 100% at 4.6×10^7 copies/mL dose. RGNNV detection and copy number also aligned with clinical outcome. Clinically affected injected fish exhibited a clear neural tropism, with brain and eyes reaching up to 10^{12} RGNNV copies/g, whereas subclinically affected injected fish displayed lower RGNNV detection frequency and copy number ($< 10^7$ copies/g). Horizonal transmission was confirmed, with 5% morbidity in cohabitated fish. Among non-destructive samples, only mucous consistently detected RGNNV (100% in clinically affected injected fish and 69.2% in subclinically affected injected fish), while urine had no detection, confirming poor diagnostic value. eRNA detected RGNNV from day 7 post-challenge, peaking after fish morbidity and reflecting active shedding rather than early detection. These findings highlighting the diagnostic value of mucous sampling and the complementary role of eRNA in surveillance of giant grouper aquaculture.

1. Introduction

Giant grouper (*Epinephelus lanceolatus*) is currently recognised as a promising aquaculture candidate due to its rapid growth rate, adaptability to diverse environmental conditions, and high market value (Glamuzina and Rimmer, 2022; Johannes, 2001). Exhibiting low food conversion ratios (0.74–0.82) and high specific growth rates (2.49–2.54%), global production of the grouper sector has increased 35.6-fold, from 7600 t in 2000 to 270,800 t in 2023 (Butler et al., 2025; FAO, 2025). Although there is potential to improve efficiency in grouper production through optimisation of aquafeed formulation and culture practices, attempts to expand the grow-out production volumes have

* Corresponding authors at: College of Science and Engineering, James Cook University, Townsville, QLD 4814, Australia.
E-mail addresses: tran.nguyenthingoc@my.jcu.edu.au (N.-T.T. Nguyen), kelly.condon@jcu.edu.au (K. Condon).

https://doi.org/10.1016/j.aquaculture.2026.744129
Received 5 March 2026; Received in revised form 5 May 2026; Accepted 6 May 2026
Available online 7 May 2026

been restricted by outbreaks of Viral Encephalopathy and Retinopathy (VER) (Thwaite et al., 2022).

VER is a major fish viral disease, affecting over 120 fish species across 54 families and exhibiting a nearly worldwide distribution in marine, freshwater, temperate and tropical systems (Bandín and Souto, 2020; Costa and Thompson, 2016). VER is caused by members of *Nodaviridae*, genus *Betanodavirus* (Mori et al., 1992). The *Nodaviridae* that cause disease in fish are colloquially termed Nervous Necrosis Virus (NNV) but formerly exist as four recognised genotypes: Red-spotted grouper NNV (RGNNV), Striped Jack NNV (SJNNV), Barfin flounder NNV (BFNNV) and Tiger Puffer NNV (TPNNV).

Groupers are primarily affected by the RGNNV genotype. NNV is neurotropic and causes vacuolation and necrosis of the nervous tissues, with specific clinical signs of VER including erratic swimming and loss of appetite. Diagnosis and detection of NNV involve assessment of brain or eye for the presence of pathognomonic lesions, virus isolation, or detection of NNV genome by reverse transcription quantitative polymerase chain reaction (RT-qPCR) (Moody and Crane, 2014). Both horizontal and vertical transmission have been reported in VER (Bandín and Souto, 2020). The high stability of the virus in seawater and its widespread distribution make prevention of the horizontal transmission pathway extremely difficult in open (cages) and semi-open (pond) grow-out aquaculture (Frerichs et al., 2000; Harikrishnan et al., 2010; Rimmer and Glamuzina, 2019). The majority of marine farmed finfish species are only adversely affected by VER during early larval development. However, some species, such as European seabass (*Dicentrarchus labrax*) and various groupers exhibit high susceptibility throughout their entire production, including grow-out (Padrós et al., 2022; Thwaite et al., 2022). Giant grouper has been reported to be affected by VER across Taiwan, China and Australia (Condon, 2019; Duan et al., 2024; Lin et al., 2001).

Although RGNNV-host-environmental interactions are presumed as the driver of disease outbreaks, limited information exists of detection and quantification of RGNNV in the environment preceding, during, or post disease outbreaks. The reliance on destructive tissue sampling, due to the neurotropic nature of RGNNV, has contributed to gaps in understanding the virus epidemiology and pathogenesis by limiting routine, repeated, and large-scale monitoring of infected fish. Consequently, evidence-based approaches to prevention of VER disease outbreaks are also limited. Understanding the drivers of natural disease outbreaks is one of the most significant hurdles to overcome to improve management of VER in aquaculture (Bandín and Souto, 2020; Costa and Thompson, 2016). Conducting a holistic approach to investigate the drivers of natural disease outbreaks, along with measuring the impact of environmental parameters in subclinically affected fish, is somewhat difficult when viral status prior to environmental influence cannot be determined without destructive sampling.

Approaches to reduce the impact of RGNNV in highly susceptible species include vaccination and genetic selection of resistant breeding lines (Yang et al., 2022). However, determining the underlying genetic and immune mechanisms that contribute to survival following VER challenge is inhibited by the inability to temporally monitor viral load and immune function in individuals as a progression with a known outcome of survival versus morbidity in highly susceptible species (Toubanaki et al., 2022). The limitation is particularly relevant for groupers, which require extended time to reach breeding maturity, making survivors valuable for breeding, but also potential RGNNV carriers, as well as for wild-caught broodstock with unknown infection status. Therefore, non-destructive approaches are needed to enable repeated monitoring of viral status without sacrificing high value fish.

Access to effective non-destructive sampling from infected fish to monitor the progression of RGNNV following experimental challenge, aligned with gene expression and survival outcome, would significantly improve the knowledge base to better manage VER. Previous studies using non-destructive tissues for NNV detection have reported limited and inconsistent diagnostic performance. In European seabass and white grouper (*E. aeneus*), gill, fin clips, and blood samples generally contained much lower viral loads than brain tissue and often produced inconsistent detection outcomes, with virus present only at certain time points (e.g., 7 days post-infection in gills and fin clips, or up to 30 days in blood) (Ferreira et al., 2019; Tarrab et al., 2019). More detailed findings indicate that sampling fin clips and scales frequently failed to detect virus even in confirmed infections (Mazelet et al., 2011; Tarrab et al., 2019), while RGNNV was only detectable in blood during a narrow infection period (5 to 15 days post infection) and mostly at high infection doses (Dalla Valle et al., 2000; Ferreira et al., 2019). Ferreira et al. (2019) reported successful RGNNV detection from non-destructive tissues, including blood, caudal fin, and gills in European seabass, but inconsistencies in viral loads and detection rates raised concerns about diagnostic reliability by returning false negatives even when infection was confirmed in brain tissue. Similarly, Padrós et al. (2022), citing Breuil et al. (1991), emphasised the limited diagnostic value of reproductive fluids in Mediterranean finfish due to irregular viral presence and technical constraints.

The ability to temporally monitor RGNNV in the environment (water) and individual fish as infection progresses has been inhibited by the reliance on destructive sampling of brain. Among non-destructive samples available from fish, analysis of mucous has been demonstrated as effective in detecting viral pathogens including infectious hematopoietic necrosis virus (IHNV) in rainbow trout (*Oncorhynchus mykiss*) (Lapatra et al., 1989), infectious salmon anaemia virus (ISAV) in Atlantic salmon (*Salmo salar*) (Griffiths and Melville, 2000), and tilapia lake virus (TiLV) in red tilapia (*Oreochromis* spp.) (Liamnimitr et al., 2018). Despite the successes in other viral diseases, the use of mucous for RGNNV detection has not been explored, highlighting the necessity for further investigation, especially in giant grouper.

In addition to the use of non-destructive samples, environmental DNA/RNA (eDNA/ eRNA) samples collected from culture water is proposed to be a simple sampling method for the surveillance of aquatic pathogens (WOAH, 2022). eRNA holds promise for the detection of viral diseases, and potentially reflects actively shed viral genetic material from infected fish, enabling the monitoring of infection dynamics in aquaculture systems (Bass et al., 2023; Farrell et al., 2021; Ip et al., 2024). Recent studies have successfully applied eRNA-based surveillance to detect iridovirus in red sea bream (*Pagrus major*) (Kawato et al., 2021) and viral haemorrhagic septicaemia virus (VHSV) in olive flounder (*Paralichthys olivaceus*) (Kang et al., 2025). Focusing on VER, RGNNV has also been detected in experimental tank water during infection in sevenband grouper (*Hyporthodus septemfasciatus*), with detection limited to fish mortality days, supporting the utility of eRNA-based surveillance for tracking viral shedding and transmission in aquaculture systems (Krishnan et al., 2021).

The current study aims to assess the suitability of non-destructive approaches for RGNNV surveillance and monitoring in giant grouper by comparing detection efficiency between destructive tissues and non-destructive samples, including mucous, urine, in clinical and subclinical fish, as well as eRNA from water. Detection efficiency is evaluated based on viral copy number and consistency of detection frequency across tissue types and clinical status, under different RGNNV doses and challenge routes. The outcomes of the current study are expected to be applied to monitor the detection of RGNNV in an aquaculture setting through improved understanding of detection performance among destructive and non-destructive sampling methods.

2. Materials and methods

2.1. RGNNV challenge extract

The RGNNV extract for experimental challenge was isolated from clinically affected orange-spotted grouper (*E. coioides*) exposed to a VER outbreak in North Queensland, Australia (Condon, 2019). Eye tissue was pooled into 100 mL sterile phosphate-buffered saline (PBS; Sigma-

Aldrich®), subjected to three freeze–thaw cycles (−25 °C to 4 °C), and homogenised with an Ultra-Turrax T25 (IKA Works) at 20,000 rpm for 5 min while kept on ice. The homogenate was clarified in a Sorval RC 6+ centrifuge (Thermo Scientific) using an F12s-6 × 500 LEX rotor, first at 610*g* for 10 min and then at 3803 g for 10 min at 4 °C. The resulting supernatant was sequentially filtered through 0.45 μm and 0.22 μm filters (Sartorius), checked for absence of culturable bacteria on sheep blood agar after overnight incubation at 28 °C, and stored at −20 °C in sterile 50 mL centrifuge tubes as the viral extract for challenge experiments.

Total nucleic acids were extracted from the viral extract using the MagMAX™ CORE Nucleic Acid Purification Kit (Applied Biosystems™) following the manufacturer's instructions. Extracted nucleic acids were analysed by RT-qPCR, which detected RGNNV-1 (RNA1 segment of the RGNNV genome) with cycle threshold (Ct) values of 24.37, corresponding to 4.6×10^8 copies/mL. This concentration was used as the viral stock for challenge studies. The stock was diluted in sterile PBS to prepare four challenge doses corresponding to 4.6×10^7, 4.6×10^6, 4.6×10^5 and 4.6×10^4 copies/mL.

2.2. Experimental giant grouper

A total of 100 juvenile giant groupers, with an average body weight of 162.6 ± 43.5 g, were obtained from a commercial hatchery. The fish were acclimated at a temperature of 26–28 °C, a salinity of 30 ppt and fed ad lib on commercial feed pellets. Prior to the experiment, RGNNV-free status was confirmed by RT-qPCR using the pooled brain and eye samples from 10 fish of the same stock.

2.3. Experimental challenge dose and design

Fish were intramuscularly injected with 100 μL of RGNNV at one of four viral doses (4.6×10^7, 4.6×10^6, 4.6×10^5 and 4.6×10^4 copies/mL) or with sterile PBS as a control. To negate any influence of water quality variation on the experimental study, the control-PBS injected fish were cohabitated with the injection challenge fish (hereafter referred to as "cohabitated fish"). Fish, grouped by dose, were placed in cages (10 fish per cage) inside two 2000 L tanks, with each tank holding five cages (one per treatment) to provide two replicates per treatment (Fig. 1). Fish were monitored every 8 h and challenges were operated for 3 weeks post-injection. To maintain stable and consistent tank conditions across treatments throughout the experiment, no water exchange was performed.

Symptomatic fish displaying VER clinical signs including loss of equilibrium, spinning, open jaw lock and lethargy were removed and euthanised (AQUI-S® at ~175 mg/L) (Coyle et al., 2004). These individuals are hereafter referred to as "clinically affected injected fish". Asymptomatic fish at the termination of experiment were also euthanised and are referred hereafter as "subclinically affected injected fish".

eRNA samples were collected from tank water by incubating a 0.22 μm mixed cellulose ester membrane filter (47 mm diameter) for two durations, 2 h and 24 h. Filters were preserved in 15 mL nuclease-free tubes filled with 2 mL MagMAX™ CORE Lysis Solution (Applied Biosystems™) and 2 mL nuclease-free water (Integrated DNA Technologies™) at room temperature (28 °C) until the further quantitative analysis (Fig. 1).

2.4. Tissue collection and extraction

Samples were collected using destructive and non-destructive methods (Fig. 1). Non-destructive samples consisted of mucous and urine collected post-euthanasia. Mucous was collected by gently swabbing the external body surface of each fish using sterile scalpel blade, while urine was collected by gently applying pressure to fish abdominal region to induce expression. Destructive samples included brain, eyes (left and right), nostril, gills, head kidney, spleen, muscle tissue at the injection site, and gut. These tissues were collected following euthanasia by aseptically excising the target tissues using sterile dissection instruments. Tissue samples were weighed and immediately placed into a 2 mL lysing matrix D tube™ (MP Biomedicals™) containing 350 μL of MagMAX™ CORE Lysis Solution (Applied Biosystems™). Tissue samples were stored at room temperature for at least 24 h prior extraction.

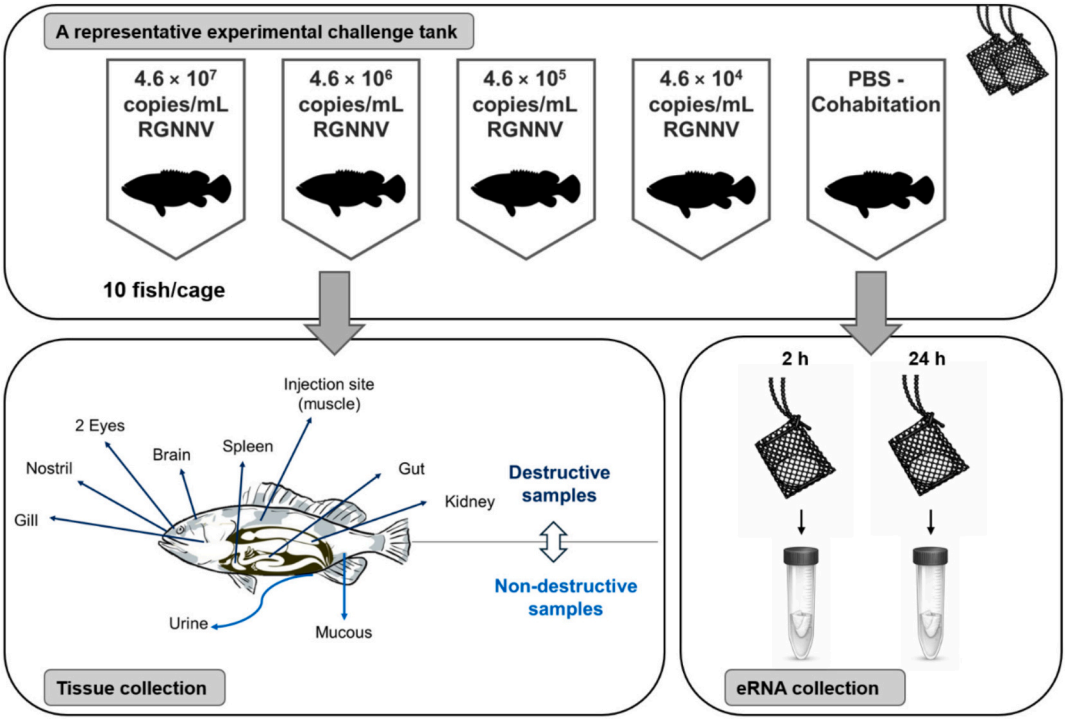

Fig. 1. Experimental challenge design and sampling workflow for RGNNV detection throughout the experiment.

2.5. Detection of RGNNV by RT-qPCR

Total nucleic acids from tissue and eRNA samples were extracted using the MagMAX™ CORE Nucleic Acid Purification Kit (Applied Biosystems™) following the manufacturer's instructions with minor modifications. For tissue samples, 5 μL of 20 mg/mL MagMAX™ CORE Proteinase K (Applied Biosystems™) was added to the sample, which was then homogenised for 30 s at 5000 rpm using a Precellys 24 tissue homogeniser (Bertin Technologies™). The homogenised samples were incubated at 72 °C for 1 h. Nucleic acids were then extracted using the KingFisher™ Flex 96 Deep-Well Magnetic Particle Processor (ThermoFisher Scientific™) and eluted in 100 μL of MagMAX™ CORE Elution Buffer (Applied Biosystems™). For eRNA samples, 375 μL of the 4 mL original lysis/water solution with filter paper was transferred to an Axygen® 1.7 mL microtube, and the remaining steps were performed as for tissue samples.

RT-qPCR was used to detect RGNNV-1 and RGNNV-2, targeting the RNA1 and RNA2 segments of the RGNNV genome, with β-actin as a host-derived protocol integrity control. The β-actin assay was originally developed from a previous teleost study (Olsvik et al., 2005) and subsequently validated through sequence alignment with giant grouper β-actin (Accession number: XM_033642591.1), confirming suitability as a host-derived marker. The master mix was prepared using the SensiFAST™ Probe Lo-ROX One-Step Kit (Meridian Bioscience™). For each reaction, 1.25 μL of sample template was added to 8.75 μL of the master mix, which included 0.5 μL of target primers (0.2 μM final concentration) and 0.5 μL of target probe (0.05 μM final concentration). Primer and probe sequences are listed in Table 1. RT-qPCR was performed on a QuantStudio™ qPCR machine (Applied Biosystems™) with the following settings: reverse transcription at 45 °C for 10 min, initial denaturation at 95 °C for 5 min, followed by 40 cycles of 95 °C for 10 s (denaturation) and 60 °C for 30 s (annealing/extension). Two positive controls and two non-template controls were included. Data was processed using QuantStudio™ Design & Analysis software (v. 1.5.1; ThermoFisher Scientific™) to generate Ct values. Samples not amplifying within 40 cycles were considered as not detected. Results of RT-qPCR to detect RGNNV from fish samples were only considered valid and included in statistical analysis if β-actin was detected within the sample.

RGNNV copy number was calculated from Ct values using a standard curve generated from ten-fold serial dilutions of a quantified RGNNV RNA standard. Ct values were converted to copy number based on the linear regression of the standard curve, and results were expressed as copies per gram of tissue. Samples in which RGNNV was not detected were assigned a viral copy number of zero per gram of tissue.

Table 1
Summary of primers and probes used for the RT-qPCR assay.

Target	Primer and probe sequence		Reference
RGNNV-1	Forward	CTT CCT GCC TGA TCC ACC TG	(Hick and Whittington, 2010)
	Reverse	GTT CTG CTT TCC CAC CAT TTG	
	Probe	CAA CGA CTG CAC CAC GAG TTG	
RGNNV-2	Forward	CCT TCG ACG CGC TTC AA	Kirkland, pers. comm.
	Reverse	TCT GCT TTC CCA CCA TTT GG	
	Probe	TCG TGG TGC AGT CGT	
β-actin	Forward	CCA AAG CCA ACA GGG AGA AG	(Olsvik et al., 2005)
	Reverse	AGG GAC AAC ACT GCC TGG AT	
	Probe	TGA CCC AGA TCA TGT TTG AGA	

2.6. Tissue-specific differences in RGNNV copy number

To investigate tissue-specific differences in RGNNV copy number, viral copy number was quantified across 10 tissue types (including brain, left and right eyes, nostril, mucous, gills, head kidney, spleen, muscle tissue at the injection site, and gut) collected from clinical and subclinical giant grouper from both injected and cohabitated groups. For injected fish, analyses were conducted using individuals challenged with high RGNNV dose (4.6×10^7 copies/mL) and two lower RGNNV dose (4.6×10^5 and 4.6×10^4 copies/mL), representing high and low viral levels. Viral copy number data were examined separately in clinical and subclinical fish to determine tissue-specific patterns of replication and their association with disease expression.

2.7. Data analysis

Morbidity data was analysed with Kaplan–Meier survival curves, and differences among challenge doses were tested by the log-rank (χ^2) test. RGNNV copy number was calculated as the average of RGNNV-1 and RGNNV-2 targets, because no significant difference was detected between the two assays ($p > 0.05$). Viral copy number data was log-transformed when necessary and analysed using non-parametric tests: Wilcoxon rank-sum for two-group comparisons (clinical status and incubation time), and Kruskal–Wallis tests with Dunn's post hoc comparisons (Bonferroni adjusted) for multiple challenge doses. Factorial effects of dose, clinical status, and tissue type were examined using aligned rank transform (ART) ANOVA, with Fish ID included as a random effect for repeated measures. Pairwise correlations among tissue groups were assessed using Spearman's rank correlation coefficients. Detection rates were summarised descriptively, and positive/negative agreement was calculated to evaluate non-destructive versus destructive tissues. All analyses were performed in R (R Core Team, 2025), with significance set at $p < 0.05$.

3. Results

3.1. Cumulative morbidity rates

Cumulative morbidity of giant grouper increased with exposure to higher viral doses during the 21-day experimental challenge (Fig. 2a). The morbidity rates followed a dose-dependent pattern, with 100% morbidity at the 4.6×10^7 copies/mL dose, followed by 90% morbidity at the 4.6×10^6 copies/mL dose, 65% morbidity at the 4.06×10^5 copies/mL dose, and 30% morbidity at the 4.6×10^4 copies/mL dose. Cohabitated fish exhibited the lowest morbidity (5%).

Despite a significant difference in cumulative morbidity, there was only a small variation in days to morbidity between the different challenge doses. Morbidity onset was first reported on day 5 in fish challenged with higher viral doses (4.6×10^7 to 4.6×10^5 copies/mL), with peak events occurring on the following days from day 6 to day 7. Given a challenge approximately 1000-fold lower than the high challenge dose, onset to morbidity was only slightly delayed to day 6, but peaked on day 7, in fish with the lowest dose (4.6×10^4 copies/mL) (Fig. 2a).

The increased morbidity recorded at higher viral doses corresponded with reduced survival. Survival analysis using the Kaplan–Meier method revealed a significant difference across viral doses with higher viral doses associated with lower survival rates, confirming the influence of viral copy number on morbidity (log-rank test: $\chi^2 = 90.3$, $p < 0.0001$) (Fig. 2b).

3.2. Detection of RGNNV using eRNA in relation to fish morbidity timeline

RGNNV was detected in experimental water using eRNA samples from day 7 post-challenge. However, RGNNV was detected two days earlier in eRNA samples incubated for 24 h compared to 2 h, indicating

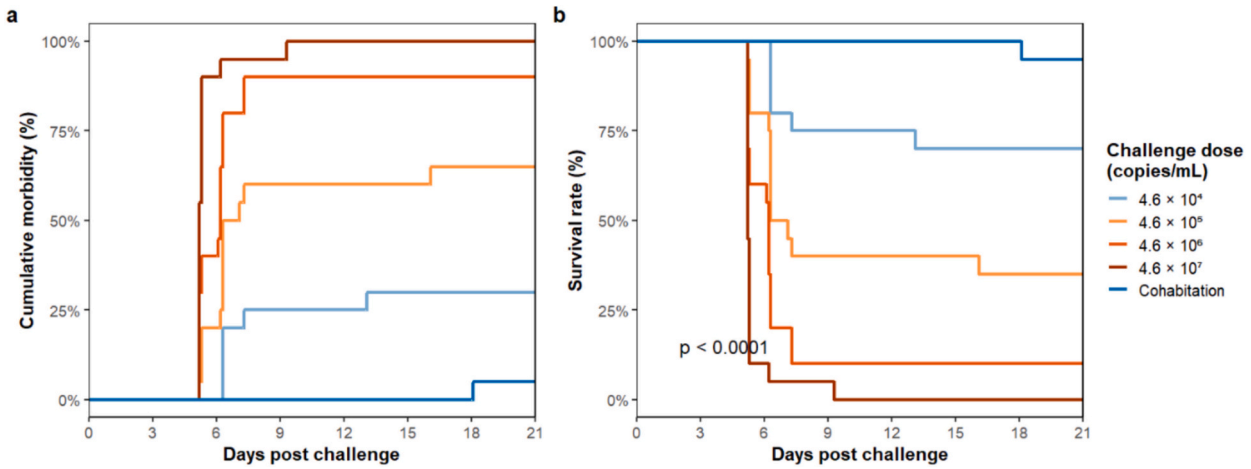

Fig. 2. Cumulative morbidity (a) and survival rate (b) of giant grouper challenged by different RGNNV doses.

that longer incubation duration may enhance the sensitivity of early detection (Fig. 3). The viral copy number increased and peaked on day 9 and 10, approximately 3–4 days after the morbidity peak, and detection continued until day 20 post-challenge (Fig. 3). Although eRNA detected RGNNV in the water, detection was delayed from the onset of disease symptoms in the fish. β-actin was also detected in water (eRNA) samples, reflecting the presence of host-derived RNA in the tank environment.

The RGNNV copy number trends differed between the two incubation times. The average viral copy number was 3668 and 8821 at 24 h and 2 h incubation, respectively. Similarly, the highest viral copy number was detected from the 2 h incubation (54,852 copies on day 11) compared to 24 h incubation (34,476 copies on day 9). Despite differences in peak of viral copy number and early detection, there was no significant difference in viral copy number detected between the two incubation times, indicating that both are equally effective for RGNNV detection in water samples during the experimental challenge ($p = 0.131$). The findings suggest that the longer incubation time may be the most sensitive approach for early detection, but shorter incubation may better preserve viral copy number RNA at peak infection; thus longer incubation could lead to viral RNA degradation or loss over time.

3.3. Results of RGNNV detection from injected challenged giant grouper

3.3.1. Frequency of RGNNV detection in different tissue types

Detection rates of RGNNV in destructive and non-destructive samples was more closely aligned with clinical outcome than challenge dose. Irrespective of challenge dose, RGNNV was detected in all destructive tissues and mucous samples from clinically affected injected fish (100% detection rates) (Fig. 4).

In subclinically affected injected giant grouper, detection rates differed across tissue types and individual fish (Fig. 4). Neither the detection rate nor tissue distribution of RGNNV followed a challenge dose dependant trend. In fish lacking clinical signs of VER, neural tissues, including brain (40.9 ± 6.4%), left eye (39.0 ± 6.4%) and right eye (34.1 ± 0.0%) exhibited the highest RGNNV detection rates, whilst nostril (31.8 ± 3.2%), gill (27.3 ± 3.2%), head kidney (15.9 ± 13.8%), and gut (13.6 ± 6.4%), had moderate detection rates. When RGNNV was detected in subclinically affected injected fish, 61.5% of fish had detection in brain, eye, and mucous, while a smaller proportion exhibited co-detection between brain and eye (15.4%) and eye and mucous (7.7%) (Fig. 5). Results indicate that RGNNV detection in mucous corresponds with infection in the neural tissues, supporting the potential of mucous as a non-destructive indicator of viral presence in subclinical fish. RGNNV was also detected only in mucous in a small proportion of fish (15.4%) (Fig. 5).

No RGNNV was detected in urine from either clinically or subclinically affected injected fish. In contrast, β-actin was consistently detected in urine samples, confirming the presence of host nucleic acids and validating sample quality and extraction.

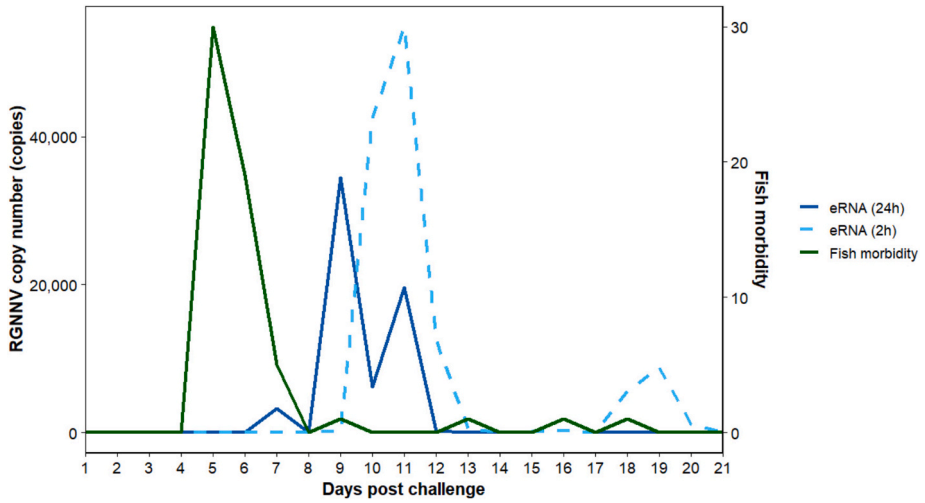

Fig. 3. Giant grouper morbidity and RGNNV copy number in eRNA samples.

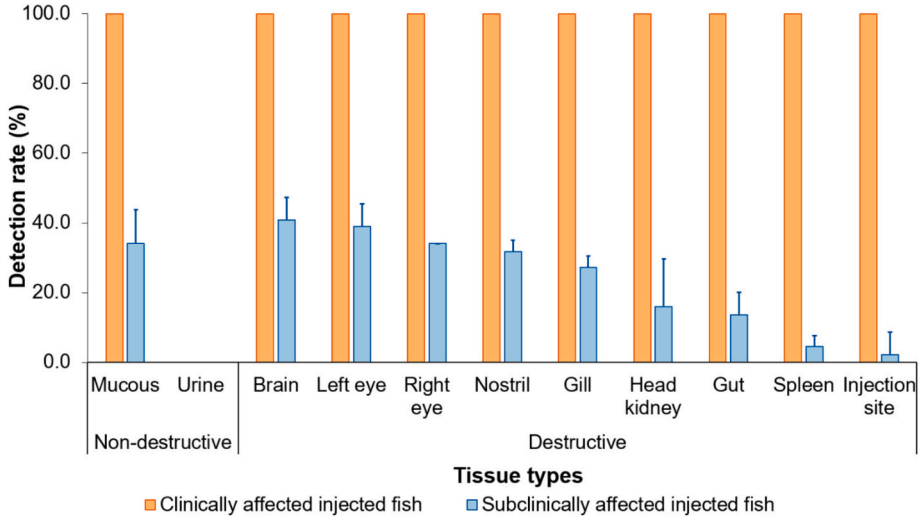

Fig. 4. RGNNV detection rate in different tissue types of clinically and subclinically affected injected giant grouper. Error bars represent variation in detection rates between RGNNV-1 and RGNNV-2.

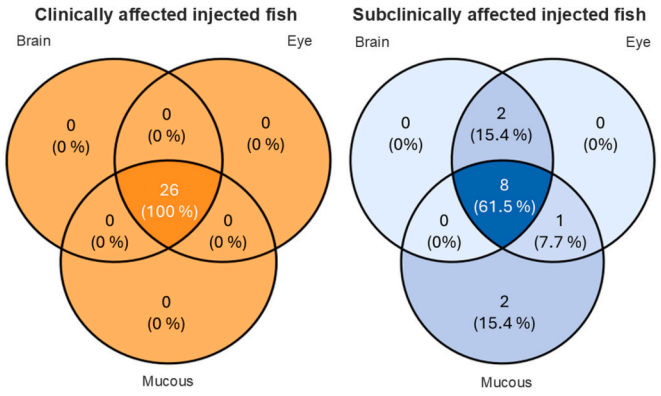

Fig. 5. Co-detection of RGNNV among brain, eye, and mucous tissues in affected injected giant grouper.

3.3.2. *Viral copy number differences across RGNNV challenge doses*

Left eye, a primary target tissue of RGNNV infection, was consistently collected from all experimental fish, providing a reliable basis for comparison across challenge doses (Moody and Crane, 2014; Munday et al., 2002). RGNNV copy number was quantified in left eyes of clinically and subclinically affected injected giant grouper across different challenge doses (4.6×10^7 to 4.6×10^4 copies/mL) (Fig. 6).

Viral copy number in left eye displayed a clear dose-dependent trend, whereby significant differences were detected across the challenge doses ($p < 0.05$). The highest RGNNV copy number (1.62×10^{12} copies/g) was detected in fish exposed to the highest challenge dose (4.6×10^7 copies/mL dose). In contrast, the lowest viral copy number (3.67×10^{11} copies/g) was recorded from fish exposed to the lowest challenge dose (4.6×10^4 copies/mL dose), while intermediate challenge doses (4.6×10^6 and 4.6×10^5 copies/mL) produced values ranging from 6.43×10^{11} to 9.26×10^{11} copies/g.

Differences in RGNNV copy number were also assessed between clinically and subclinically affected injected fish. Clinically affected

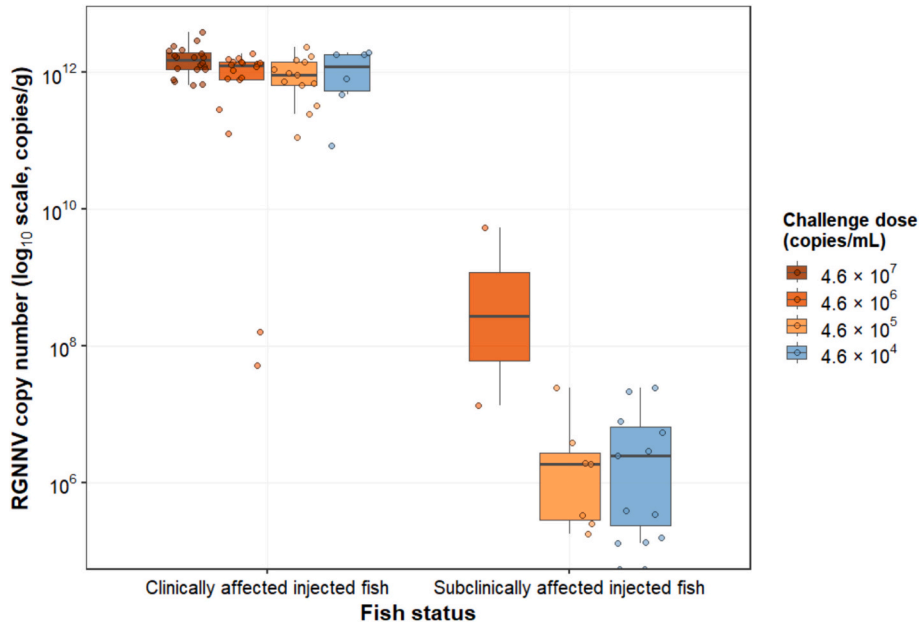

Fig. 6. RGNNV copy number ($\log_{10}$ scale, copies/g) in left eye of clinically and subclinically affected injected giant grouper across challenge doses.

injected fish had significantly higher viral copy number (average 1.24×10^{12} copies/g) than subclinically affected injected fish (average 2.53×10^{8} copies/g) ($p < 0.05$), confirming a strong association between viral copy number and disease expression. However, there was no significant interaction between challenge dose and clinical status ($p > 0.05$). As noted, no subclinically affected injected fish were recorded at the highest challenge dose (4.6×10^{7} copies/mL).

3.3.3. RGNNV copy number differences across tissue types

RGNNV was detected in variable copy number in different tissues (Fig. 7). RGNNV copy number displayed a distinct trend with clinical outcome whereby RGNNV was detected in higher copy number in all tissues in fish which displayed clinical signs of VER compared to those with no clinical signs. Difference in RGNNV copy number was significant and influenced by both tissue type and viral dose with a strong interaction between tissues and challenge doses ($p < 0.001$).

In clinically affected injected fish, viral copy number displayed a consistent pattern in which neural tissues (brain, left eye and right eye) carried the highest viral copy number across all challenge doses (4.6×10^{7}, 4.6×10^{5}, and 4.6×10^{4} copies/mL) (Fig. 8). In contrast, non-neural tissues exhibited more variable dose-dependent patterns. Viral copy number in non-neural tissues was highest from external epithelial surfaces (nostril and body mucous), while RGNNV detections in spleen, head kidney and gut were comparatively reduced in clinically affected injected fish.

Only fish that were challenged with lower doses (4.6×10^{5} and 4.6×10^{4} copies/mL) survived and were analysed as subclinically affected injected fish. In the absence of clinical signs, RGNNV was detected with lower frequency and lower viral copy number in different tissue types (Fig. 7). RGNNV copy number in subclinically affected injected fish ranged from 8.46×10^{3} to 4.53×10^{7} copies/g (Fig. 9).

RGNNV copy number in tissues from clinically affected injected giant grouper

In clinically affected injected fish, pooling across challenge doses, viral copy number differed significantly among tissue types ($p < 0.001$) (Fig. 8). Neural tissue (brain, right eye and left eye) exhibited the highest viral copy number, with average values of 6.16×10^{12}, 1.64×10^{12} and 1.34×10^{12} copies/g, respectively. Post hoc analysis concluded neural tissues formed a distinct group, significantly higher than all non-neural tissues. RGNNV copy number in non-neural tissues were lower than neural tissues, ranging from 2.06×10^{8} to 5.43×10^{9} copies/g. Among non-neural tissues, mucosal and epithelial tissues, particularly nostril (5.43×10^{9} copies/g) and mucous (2.07×10^{9} copies/g), had the highest viral copy number. Immune tissues, including head kidney (1.32×10^{9} copies/g) and spleen (4.63×10^{8} copies/g), exhibited intermediate values, whereas internal tissues such as gut (3.97×10^{8} copies/g) and injection site (2.06×10^{8} copies/g) had the lowest viral copy number.

RGNNV copy number in tissues from subclinically affected injected giant grouper

In subclinically affected injected fish, pooling across challenge doses, viral copy number differed significantly among tissue types ($p < 0.001$) (Fig. 9). The highest viral copy number (1.65×10^{6} to 4.53×10^{7} copies/g) were detected in neural tissues (brain and two eyes), nostril and gill. Among non-neural tissues, mucous displayed intermediate viral copy number (4.03×10^{5} copies/g), while immune tissues (head kidney and spleen) had lower viral copy number averaging 4.77×10^{5} and 1.45×10^{5} copies/g, respectively. Injection site exhibited the lowest viral copy number (8.46×10^{3} copies/g). Post hoc analysis indicated RGNNV copy number was not significantly different between mucosal and neural tissue but otherwise exhibited a similar trend to the post hoc analysis from clinically affected injected fish. Notably, in clinically affected injected fish, the average RGNNV copy number exceeded 10^{7} copies/g in all tissue types, yet a similar 10^{7} copies/g threshold was detected in the brain of subclinically affected injected fish.

RGNNV correlation across tissue types

Pairwise correlation analysis revealed strong associations in RGNNV copy number among major tissue groups (Fig. 10). Tissues were categorised into neural (brain and eyes), mucosal (mucous, nostril, gill, and gut), immune (head kidney and spleen), and other tissues (injection site). Significant positive correlations were investigated between neural, immune, and mucosal tissues, indicating that viral replication across sites followed a similar trend. The strongest relationships occurred between neural and mucosal tissues ($r = 0.77$, $p < 0.001$), immune and neural tissues ($r = 0.77$, $p < 0.001$), and immune and mucosal tissues ($r = 0.73$, $p < 0.001$). A moderate correlation was detected between other and mucosal tissues ($r = 0.62$, $p \leq 0.001$), while weak and non-significant correlations were found for other and immune ($r = 0.38$, $p = 0.052$), and other and neural tissues ($r = 0.35$, $p = 0.081$).

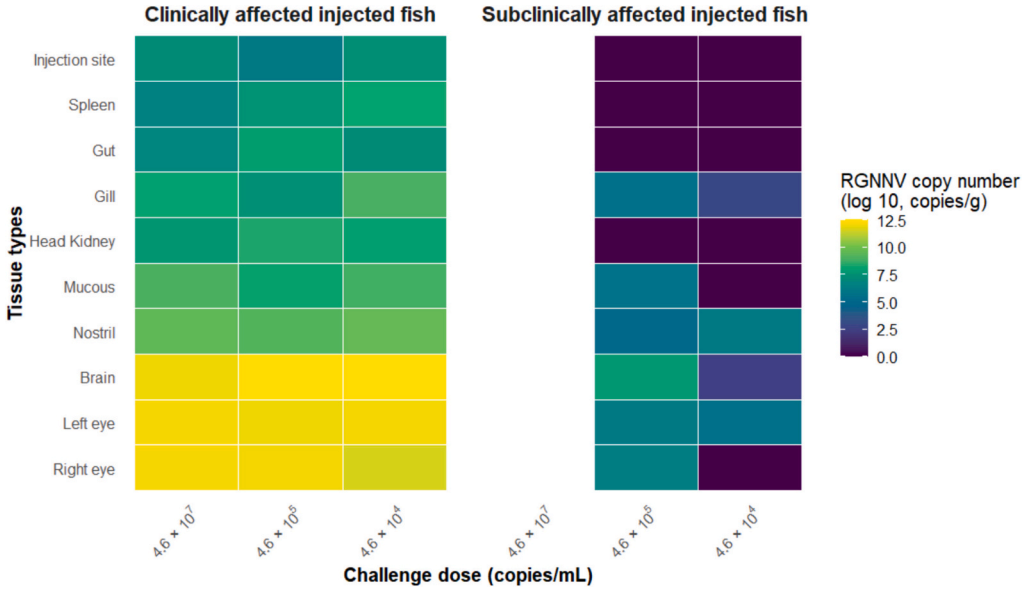

Fig. 7. Tissue-specific distribution of RGNNV copy numbers (log_{10} scale, copies/g) in clinically and subclinically affected injected giant grouper under different challenge doses. Colour intensity reflects relative viral abundance across tissues and doses.

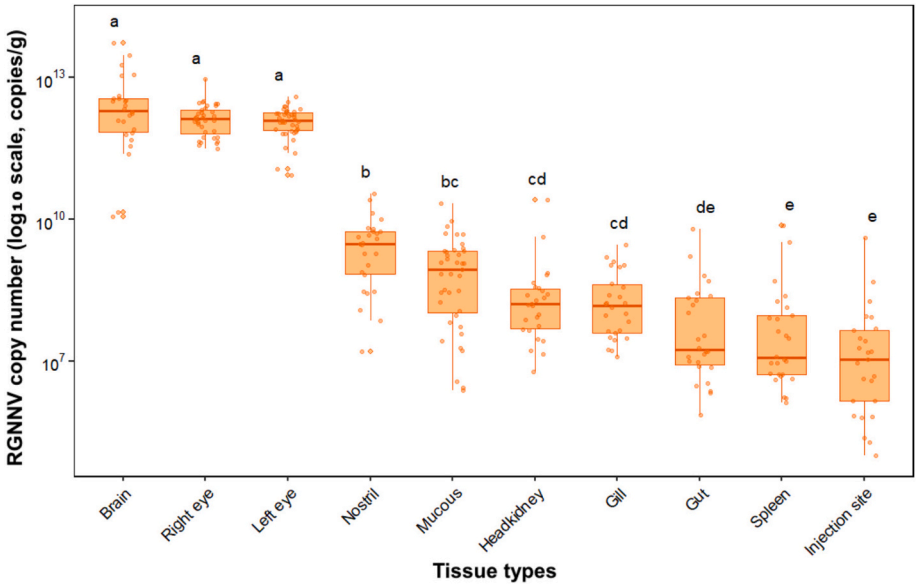

Fig. 8. RGNNV copy number (log_{10} scale, copies/g) across different tissue types in clinically affected injected giant grouper. Different superscript letters (a – e) indicate significant differences among tissues ($p < 0.05$).

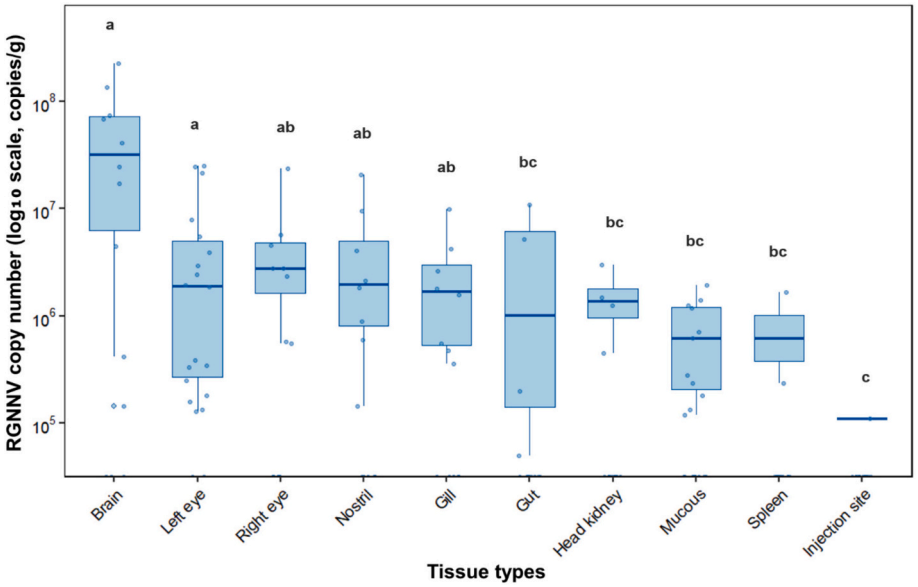

Fig. 9. RGNNV copy number (log_{10} scale, copies/g) across different tissue types in subclinically affected injected giant grouper. Different superscript letters (a – c) indicate significant differences among tissues ($p < 0.05$).

3.4. Results of RGNNV detection from cohabitated giant grouper

3.4.1. Frequency of RGNNV detection in different tissue types

Cohabitated giant grouper, which were not directly injected with RGNNV but shared same culture tanks with injected challenged fish, exhibited varying levels of viral detection. Only one of the 20 cohabitated fish became moribund while the other 19 fish remained subclinical. RGNNV was detected in all tissue of the moribund individual, whereas the subclinical cohabitated fish had variable detection rates (Fig. 11). Within the subclinical cohabitated fish, RGNNV was detected in 18 (90%) of the cohabitated fish, with approximately 50% having detection restricted to neural tissues. One fish had no RGNNV detection in any tissue, indicating potential resistance to infection. The findings highlight that although horizontal transmission was effective, morbidity and distribution of RGNNV in tissues differed among individuals. Left eye exhibited the highest RGNNV detection rate (89.5%), followed by mucosal tissues such as mucous, gut, and gill (each 31.6%). Lower detection of RGNNV occurred in right eye (21.1%), nostril (15.8%), brain (15.8%), and spleen (10.5%), while urine, head kidney, and injection site consistently had no detection.

3.4.2. RGNNV copy number in cohabitated fish

Similar to the injected challenged fish, cohabitated fish displayed a clear separation in viral copy number between clinical and subclinical individuals (Fig. 12). The VER clinical cohabitated fish carried high viral copy number (3.09×10^{11} copies/g), whereas subclinical cohabitated fish had significantly lower copy number (6.20×10^{5} copies/g, $p < 0.05$). The RGNNV copy number of 3.09×10^{11} copies/g, was slightly lower, but not significantly different from clinically affected injected fish (9.02×10^{11} copies/g, $p = 0.910$). In contrast, subclinical

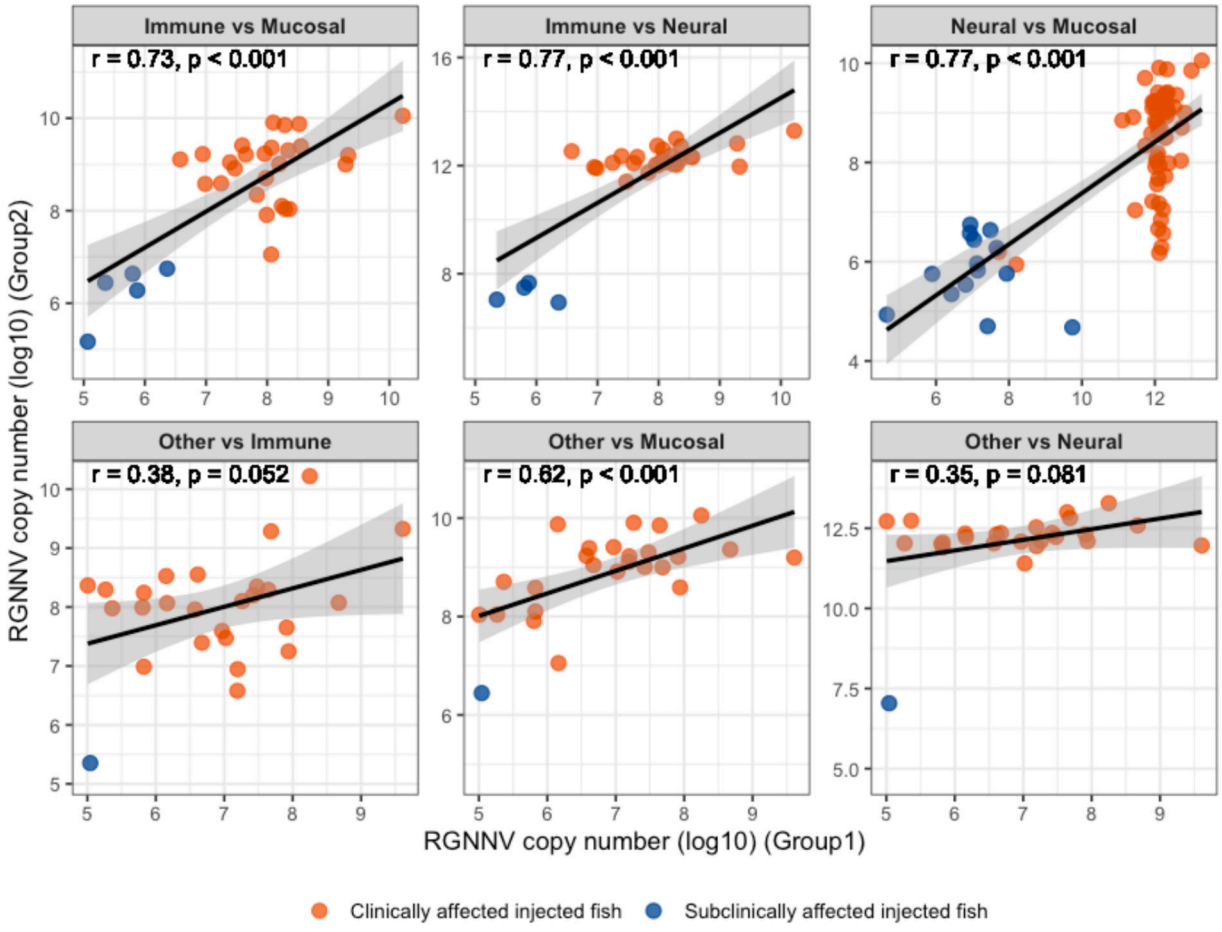

Fig. 10. Pairwise correlations of RGNNV copy number among tissue groups in affected injected giant grouper. Tissue categories include neural (brain, left eye and right eye), mucosal (mucous, nostril, gill, and gut), immune (head kidney and spleen), and other tissues (injection site).

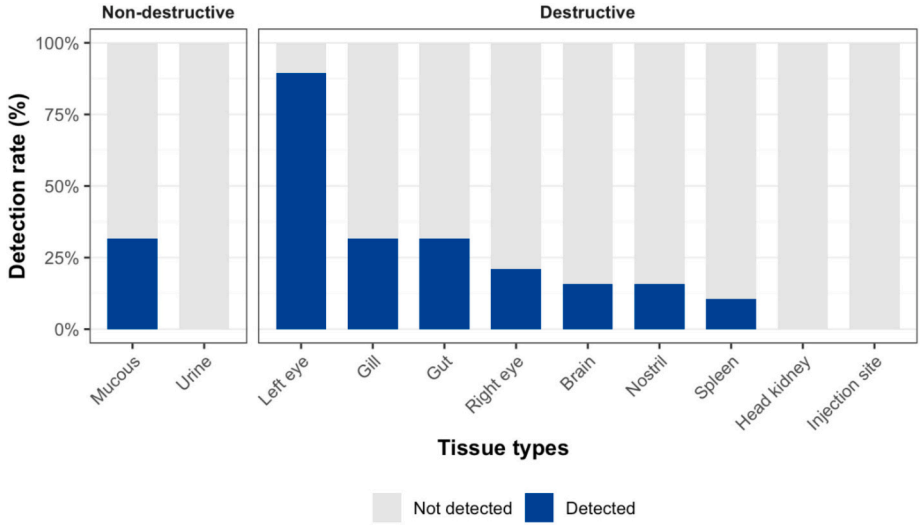

Fig. 11. RGNNV detection rates in different tissue types of subclinical cohabitated giant grouper.

cohabitated fish exhibited significantly lower viral copy number (6.20 $\times$ 10^5 copies/g) than subclinically affected injected fish (4.26 $\times$ 10^7 copies/g, $p < 0.05$). Across both injected and cohabitated groups, clinical fish tended to have smaller body weight (139.7 $\pm$ 26.4 g) than subclinical fish (191.4 $\pm$ 37.6 g), suggesting that body weight may reflect host condition and disease progression relevant to tissue-level viral replication.

RGNNV copy number in subclinical cohabitated fish revealed a distinct concentration in neural tissues (Fig. 13). Left eye carried the highest copy number (4.96 $\times$ 10^6 copies/g) among tissues. Right eye (1.63 $\times$ 10^5 copies/g) and brain (6.63 $\times$ 10^4 copies/g) also contained detectable RGNNV, indicating that neural tissues remained the primary

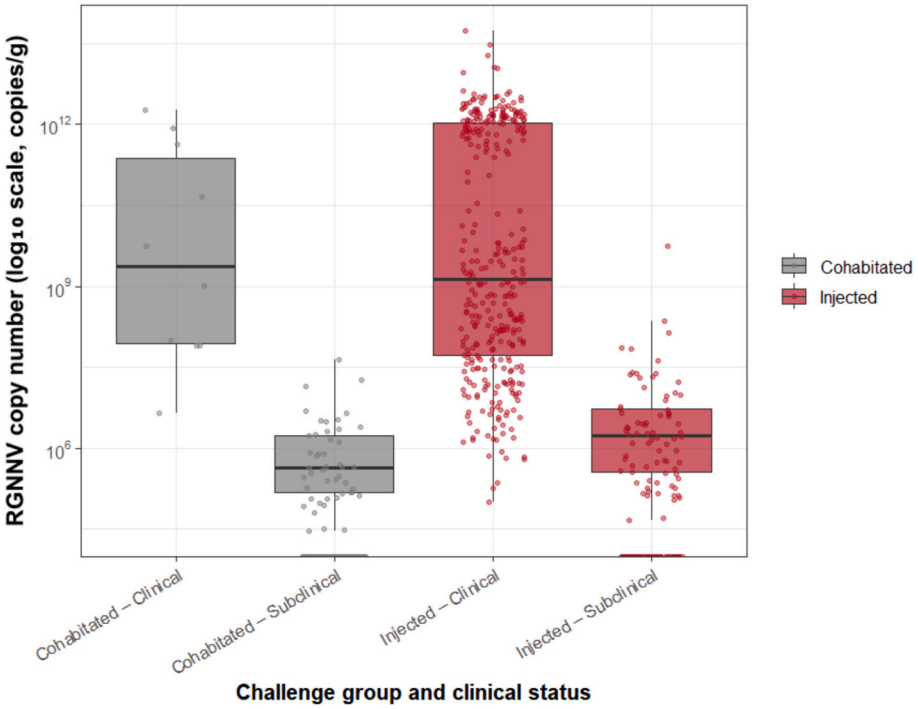

Fig. 12. RGNNV copy number (log_{10} scale, copies/g) in all tissues across challenge group and clinical status in giant grouper.

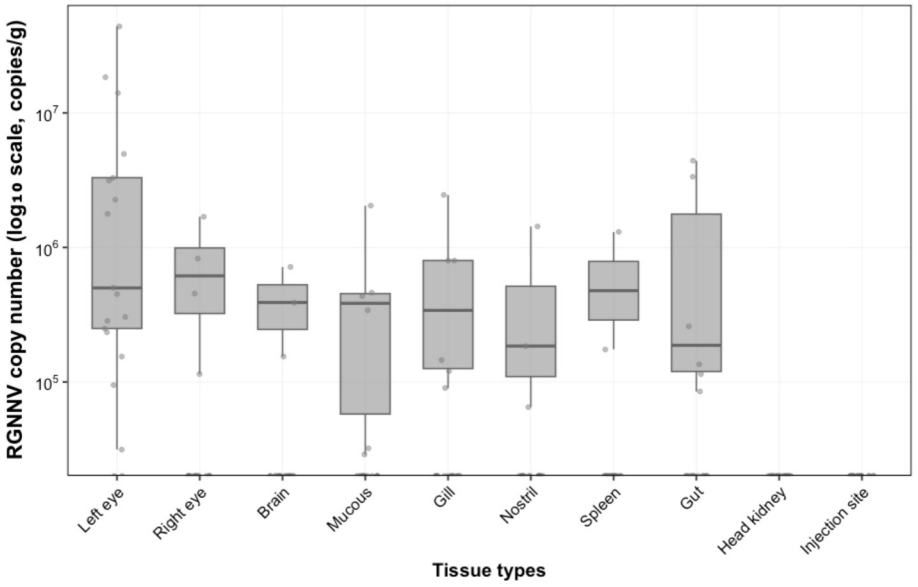

Fig. 13. RGNNV copy number (log_{10} scale, copies/g) across different tissue types in subclinical cohabitated giant grouper.

sites of persistence even in the absence of VER clinical signs. Outside the nervous system, viral copy number was lower. Gut (4.39×10^5 copies/g), gill (2.32×10^5 copies/g), and mucous (1.76×10^5 copies/g) had the highest viral copy number among non-neural tissues, while nostril and spleen contained only low copy number (8.84×10^4 and 7.76×10^4 copies/g). RGNNV was not detected in the head kidney and injection site.

In summary, viral copy number in subclinical cohabitated fish indicates that subclinical infections involve low tissue distribution of RGNNV, with viral replication concentrated primarily in the eye and secondarily in the brain. Viral copy number in mucosal, immune, and internal tissues were minimal. Collectively, the differential RGNNV detection patterns across tissue types, sampling methods, infection routes, and clinical status, are summarised in Table 2.

4. Discussion

Effective surveillance of viral diseases in aquaculture is limited by the lack of reliable non-destructive sampling approaches and insufficient understanding of how virus detection varies among tissues during clinical status (Brugere et al., 2017). For VER, diagnostic sensitivity is highest in neural tissues; however, reliance on destructive sampling restricts repeated monitoring and limits detections of subclinical infections within aquaculture settings. Although interest in non-destructive sampling is increasing, direct evaluation of destructive versus non-destructive sampling methods remains limited, and the

Table 2
Summary of RGNNV detection patterns across sampling methods, tissue types, infection routes, and clinical status.

Sampling method	Tissue category	Tissue type	Infection route	Clinical status	Detection rate (%)	RGNNV copy number (copies/g)	Diagnostic relevance
Destructive	Neural	Brain and eyes	Injection	Clinical	100	10^{12}	Primary target tissue
				Subclinical	34.0–40.9	10^{6}–10^{7}	Key target tissue for subclinical detection
			Cohabitation	Clinical	100	10^{11}	Systemic infection confirmation
				Subclinical	15.8–89.5	10^{3}–10^{6}	Primary persistence site
	Non-neural	Nostril, gill, head kidney, spleen, injection-site muscle and gut	Injection	Clinical	100	10^{8}–10^{9}	Secondary tissues
				Subclinical	13.6–31.8	10^{3}–10^{5}	Limited diagnostic value
			Cohabitation	Clinical	100	10^{9}	Secondary sites
				Subclinical	0–31.6	0–10^{5}	Minimal involvement
Non-destructive	Non-neural	Mucous	Injection	Clinical	100	10^{9}	Reliable non-destructive alternative
				Subclinical	34.1 ± 9.6	10^{5}	Promising non-destructive indicator
			Cohabitation	Clinical	100	10^{9}	Shedding indicator
				Subclinical	31.6	10^{5}	Surveillance tool
		Urine	All	All	0	0	Not suitable
Environment	–	eRNA	–	Tank level	Delayed detection	Peak after fish morbidity	Shedding signal only

relationship between viral detection in alternative samples and infection status is poorly characterised in giant grouper. Addressing this limitation, the current study demonstrates that RGNNV detection in giant grouper is strongly tissue-specific and that non-destructive sampling, particularly mucous-based detection, can reliably detect infection across both clinical and subclinical status, while eRNA provides complementary tank-level surveillance.

4.1. Tissue-specific detection of RGNNV and implications for diagnosis

A key finding of the current study was the strong tissue-specific pattern of RGNNV detection across experimental fish, with viral copy number varying markedly across different tissue types. Confirming pre-established knowledge, the key trend at the tissue level was the strong concentration of RGNNV replication in neural tissues. Across all VER affected injected fish, brain and eyes consistently exhibited distinctly higher viral copy number than all other tissues. In clinically affected injected fish, viral copy number in neural tissues were approximately 10^{2}–10^{3}-fold higher than those in mucosal tissues and up to 10^{4}-fold higher than those in internal tissues. Non-neural tissues carried lower and more variable viral copy number, suggesting secondary involvement in infection process. Mucosal and epithelial tissues, including nostril, mucous, gill, and gut, exhibited intermediate viral copy number, higher than those found in immune tissues (kidney and spleen). Detection of RGNNV in tissues with direct contact with water align with known horizontal transmission pathways of RGNNV, where waterborne contact with infected fish or contaminated material brings external surfaces into direct contact with infectious particles (Munday et al., 2002; Yang et al., 2022). Although direct evidence for RGNNV entry through mucosal surfaces is limited, studies on other fish viruses indicate mucosal epithelia can act as important contact points during early exposure. Some viruses can bind alternative epithelial receptors and cross mucosal barriers (Bergelson, 2003). For example, ISAV has been recorded to infect epithelial cells of the gill, skin, and gastrointestinal tract during early infection (Aamelfot et al., 2015). The precise receptors that facilitate internalisation of NNV particles have not been determined but proposals include epithelially expressed Heat shock protein 70 (HSP70) and HSP90ab1 as well as the adhesion proteins Nectin types 1 and 4 (Krishnan et al., 2019; Zenke and Okinaka, 2022; Zhang et al., 2024). Interestingly, tissue distribution of viral copy number observed in the current study reflects the trend of Nectin-1 detection observed in *E. lanceolatus* x *E. fuscoguttatus* hybrids with brain, eye and gill exhibiting highest Nectin 1 expression compared to spleen, liver, muscle, head kidney and intestine (Zhang et al., 2024).

Correlations among tissue types indicate viral replication was observed across neural, mucosal, and immune tissues. Strong positive correlations between neural and mucosal tissues, and between neural and immune tissues, indicate that viral copy number in these tissues are closely linked once infection is established. Experimental infections have shown that nodaviruses can spread systemically across different fish tissues. For example, in Atlantic halibut, nodavirus was detected in kidney, heart, liver, and intestine with increasing viral loads over time and confirmed replication in brain and retina (Grove et al., 2003). Sevenband grouper exhibited similar patterns, with NNV detected in all sampled tissues and high burdens in fish brain and eye (Kim et al., 2018). Atlantic cod (*Gadus morhua*) exhibited similarly broad tissue distribution with marked replication in brain and retina (Korsnes et al., 2009). Although tissue distribution of nodaviruses has been described previously, correlations among tissue groups have not been investigated. Correlations observed in the current study should be considered when investigating transcriptomic response to RGNNV challenge.

Interestingly, although detection of RGNNV reflected a similar pattern of tissue distribution across both challenge routes (e.g. injected and cohabitation), a notable difference of an absence of detection of RGNNV from head kidney and the muscle/skin injection site was observed from cohabitated fish. Results of RGNNV detection from head kidney samples in injection challenged fish is potentially an artefact in tissue distribution driven by a challenge route that bypasses the mucosal immune pathway. Alternatively, the variable detection of RGNNV within each challenge dose may be indicative of individual variation in the early antiviral activity in the head kidney to rapidly activate interferon-mediated responses that clear circulating virus before detectable replication can occur (Chen et al., 2014; Yong et al., 2017). In which case, absence of RGNNV in the head kidney of cohabitated fish may reflect also limited systemic distribution, where viral replication in neural tissues does not reach the threshold required for dissemination to internal immune organs (Costa and Thompson, 2016; Grove et al., 2006). The dominance of detection in the eye and mucosal surfaces, together with the absence of RGNNV in urine and head kidney, suggests that infection in cohabitated fish arose through waterborne exposure, with initial viral entry via ocular or mucosal tissues. The strong concordance of mucous analysis with brain and eye suggests analysis of mucous following natural or experimental exposure may serve as a useful tool to screen for individuals with resistance to RGNNV in experimental challenge or natural disease outbreaks. Further investigation into RGNNV in mucous samples is warranted and proteomic analysis may identify mucosal factors that influence RGNNV detection in individuals.

4.2. Performance of non-destructive sampling approaches for RGNNV surveillance

The distribution and RGNNV copy number across tissues, doses, challenge route and clinical outcome inform the diagnostic utility of different tissues, which can be better understood, supporting the assessment of non-destructive sampling methods for RGNNV detection. To date, no prior studies have investigated the diagnostic value of non-destructive samples in clinically and subclinically affected grouper. Therefore, the current study offers the first evidence of the potential value of mucous and urine for RGNNV detection. Urine had no detectable RGNNV, despite good sample quality. The non-detection of RGNNV in urine eliminates the usefulness of the urine sample as a monitoring tool but also indicates the biological mechanism of viral shedding from infected individuals to drive the horizontal transmission pathway does not occur via urination. The current study found mucous to be a promising candidate for RGNNV detection as a diagnostic tool during disease outbreaks and to detect subclinically infected fish in a surveillance application. Mucous displayed strong diagnostic performance among the non-destructive tissue with 100% detection in clinically affected injected fish and strong concordance (69.2%) with neural tissues in subclinically affected injected individuals. Further to being useful as a sample for detection, the RGNNV copy number detected in the mucous samples also displayed high correlation with copy number from neural tissues. To our knowledge, this is the first report of diagnostic value of mucous to detect RGNNV; however, the diagnostic value of mucous is reported from other fish viral diseases. Infectious particles of salmonid alphavirus (SAV) were detected by RT-qPCR and isolated from mucous of Atlantic salmon which were experimentally challenged by intraperitoneal injection (Graham et al., 2012). More recently, TiLV was detected in mucous from 21 field samples demonstrated to be infected with TiLV using liver samples (Liamnimitr et al., 2018). Mucous allowed earlier detection than internal tissue for both IHNV and TiLV and detected viral infections in fish without clinical signs in ISAV and SAV carriers (Griffiths and Melville, 2000; Liamnimitr et al., 2018). Although the concordance between mucous and neural tissues was high (69.2%), further work should be conducted to determine if increasing testing replicates improves accuracy of detection compared to brain or eye tissues. As a practical outcome, the current study indicates mucosal screening of fish that survive an RGNNV outbreak will provide a strong indication of whether the fish is a carrier of RGNNV or has cleared RGNNV. In a farming scenario, knowledge of carrier versus cleared status would assist with management decisions to retain survivors as valuable broodstock. In a scientific application, the ability to determine status of groupers following RGNNV experimental challenge enables subsequent studies to investigate the longevity of RGNNV detection, apply a holistic approach that measures the impact of environment on immune response and RGNNV in survivors, and investigate genetic markers for resistance.

4.3. eRNA detection for RGNNV surveillance

The current study also evaluated eRNA as a non-destructive method for detecting RGNNV in water. RGNNV was successfully detected by eRNA in experimental challenge systems; however, detection lagged disease progression. Morbidity in challenged fish peaked at 6–7 days post-challenge, whereas RGNNV was first detected in water 2–3 days later and remained detectable until day 20 post-challenge, albeit at substantially lower copy number. The current study indicates that eRNA detection of RGNNV reflects established infection rather than providing early pathogen detection. The temporal detection of RGNNV in the environment only after morbidity is consistent with previous studies. In sevenband grouper, RGNNV was detectable in tank water only on days when mortality occurred, suggesting that waterborne viral RNA primarily reflects active clinical infection (Krishnan et al., 2021). Similarly, for VHSV in olive flounder, eRNA concentrations in seawater closely aligned with mortality curves (Kang et al., 2025). Collectively, studies suggest that while eRNA is valuable for confirming ongoing viral activity at the population level, its utility for early warning is constrained by the requirement for substantial viral shedding. However, the ecological and epidemiological conditions that lead to natural outbreaks of VER remain poorly defined. The drivers of VER outbreaks have not been identified from field studies. Based on viral dose challenge, a high viral dose exposure is required to induce VER. Additional factors such as significant immune depression in groupers may also be a contributing factor to natural disease outbreaks, however no such event has been reported in the literature. Therefore, the induction of VER in an experimental challenge model may influence shedding dynamics and RGNNV detection timing. In a natural disease outbreak, it is plausible that RGNNV shedding by vectors or subclinically infected hosts could precede substantial disease under natural conditions and be detectable via eRNA. The current conclusions may reflect viral shedding kinetics inherent to the experimental design rather than limited sensitivity of the eRNA methodology. The current study has demonstrated proof of concept of eRNA to detect RGNNV; however, field-based investigations are required to clarify the predictive value of eRNA surveillance in a commercial aquaculture setting.

Detection of RGNNV in water via eRNA also provides insight into infection dynamics in cohabitated fish. In the current study, only a single cohabitated fish became moribund. Morbidity occurred at day 17 post-challenge, approximately 11 days after the peak morbidity in injected challenged fish and approximately 9 days after the first detection of RGNNV in the water using eRNA. Viral theory suggests the low infection prevalence and morbidity among cohabitated fish were likely due to low dose exposure to RGNNV via water attributable to the humane removal and euthanasia of clinically affected injected individuals, thereby limiting viral shedding. Similar reductions in morbidity following removal of infected fish have been reported in RGNNV challenge study in European seabass (Ferreira et al., 2019). The combined results of RGNNV detection from mucous and eRNA data support two key inferences: RGNNV shedding and infection occur through mucous and markedly increase only after clinical disease onset, which implies the management strategy of prompt removal of clinically affected fish should substantially reduce environmental viral loads. In an aquaculture setting, reduced loading of RGNNV in the environment, particularly at the start of a disease outbreak, should theoretically reduce severity of the disease outbreak. The conclusions align with anecdotal industry observations that removal of VER-affected fish during outbreaks reduces disease severity. The low viral shedding until viral infection is well advanced also sheds some insight into why RGNNV infections can lead to such high mortality in an aquaculture setting. In fish, innate responses often arise only after viral replication is already increasing, giving high-dose exposures a substantial early advantage and allowing infection to progress rapidly (Ortega-Villaizan et al., 2022; Poisa-Beiro et al., 2008). The release of large viral copy number with peak infection rather than slow gradual release as infection progresses potentially results in numerous virions achieving fish receptor binding simultaneously creating multiple invasion points and potentially reducing the efficacy of numerous focal immune responses to prevent RGNNV infection. Once high tissue invasion is achieved, because RGNNV is strongly neurotropic, high infectious doses are more likely to reach pathogenic thresholds sooner than low doses, contributing to the faster onset and severity typically observed in RGNNV infections (Munday et al., 2002).

4.4. Dose-dependent infection and VER disease outcomes

Within the diagnostic context, the current study observed the clear dose-dependent infection response in giant grouper challenged via intramuscular injection with RGNNV, reflected in morbidity patterns, viral replication intensity and tissue distribution. The trends observed in the current study align with viral-kinetics and host–pathogen theory, which predict that higher infectious doses promote more rapid viral

amplification, overwhelm early innate antiviral defences, and accelerate the progression of infection (Alizon et al., 2009; Wargo et al., 2017). Fish exposed to higher RGNNV doses by injection developed clinical signs earlier and with much greater frequency than those challenged with lower doses which produced delayed onset or subclinical outcomes. Similar dose-dependent patterns have been reported in other RGNNV susceptible species. Sevenband grouper, challenged with high intramuscular doses (10^{-1} and 10^{-2}), exhibited rapid onset of abnormal swimming and 100% mortality within 6 days, whereas challenge with more diluted doses (10^{-3} to 10^{-5}) resulted in weaker or delayed clinical signs (Tanaka et al., 1998). An intraperitoneal challenge in the same species also reported a graded mortality response ranging from 35% at 10^3 $TCID_{50}$ to 80% at 10^5 $TCID_{50}$ (Krishnan et al., 2021). Likewise, Australian bass (*Macquaria novemaculeata*) only developed clinical signs when exposed to immersion doses of 10^3 $TCID_{50}$/mL or higher, while lower doses produced partial or no infection (Jaramillo et al., 2019). Across studies and species, including the current study, central role of viral dose in determining VER disease severity is consistently evident and aligns with biological theory of high challenge dose exceeding immune threshold leading to disease expression.

Also consistent with dose-dependent patterns, a major difference between infection outcomes with higher RGNNV copy number and RGNNV detected from more tissues in clinically affected injected fish compared with subclinically affected injected individuals was revealed. Clinically affected injected fish exhibited viral copy number approximately 5×10^3-fold higher than subclinically affected injected fish, indicating that progression to VER occurred only when viral replication rose to extremely high levels (i.e., approximately 10^{11} copies/g in neural tissues in this study). In contrast, subclinically affected injected fish, injected with RGNNV and surviving to the end of the experiment, carried detectable but low viral copy number. Interestingly, the absence of clinical signs did not reflect a lack of infection, but rather comparatively lower viral copy number. A comparable 10^4–10^6-fold difference has been reported for VHSV infection in olive flounder, in which moribund fish exhibited higher viral copy number (10^{10} copies/mL) than survivors (10^4–10^6 copies/mL) (Kim et al., 2019). The current study noted clinical disease occurs with very high copy number in neural tissues and RGNNV detection in all tested tissues with average copy number of RGNNV exceeding a threshold of 10^7 copies/g tissue. In contrast, systemic detection of RGNNV in all tissues did not occur in subclinically affected injected fish.

Detection of RGNNV in cohabitated fish confirmed waterborne transmission of RGNNV within the challenge system. The current study observed differences in viral copy number, tissue distribution and survival-disease outcome in cohabitated versus injected challenged fish, emphasising that both viral dose and infection pathway influence the progression of RGNNV pathogenesis. Cohabitation outcomes further supported infection-intensity patterns under natural transmission. The copy number of RGNNV in the single moribund cohabitated fish reached viral copy number (3.09×10^{11} copies/g) similar to clinically affected injected fish (9.02×10^{11} copies/g) as well as systemic infection. In contrast, subclinical cohabitated fish carried 70-fold lower viral copy number than subclinically affected injected fish and reduced tissue distribution, consistent with more limited viral uptake under natural horizontal exposure. Waterborne transmission was also recorded in sevenband grouper, where virus was detected in tank water during shedding periods and cohabitated fish were infected through environmental exposure alone (Krishnan et al., 2021). A similar transmission pathway occurred in Atlantic halibut (*Hippoglossus hippoglossus*), where exposure to virus-contaminated water led to systemic infection confirmed by RT-qPCR and histopathology (Grotmol et al., 1999). These findings support the interpretation that cohabitated fish in the current study became infected via waterborne viral shedding.

The results agree with previous conclusions that clinical disease develops when viral replication exceeds a copy threshold (Lancaster and Pfeiffer, 2012). To date, few studies have quantified viral copy number in both clinically and subclinically affected fish following RGNNV challenge. Disease with high viral copy number outcome aligns with early innate responses determining infection outcome, as inadequate initial rapid control of the virus enables rapid replication and disease, whereas effective early restriction of viral replication restricts infection to subclinical levels (Avunje et al., 2011; Guo et al., 2019). However, the large fold difference observed in the current study also provides useful insight into the replication thresholds linked to VER. Results suggest that clinical disease is influenced not only by exposure dose. Despite different challenge dose, all clinically affected injected individuals displayed similar viral copy number in neural tissues. Conversely, within the lower challenge dose, variable survival, detection and viral copy number was observed across individual fish.

Despite identical challenge doses and exposure conditions, substantial variation in infection outcomes was observed among individual fish at lower challenge doses and under cohabitation conditions. Fish challenged by injection with high dose demonstrated high morbidity and high viral copy number as a systemic infection in multiple tissues. In contrast, fish challenged at lower doses and through cohabitation conditions displayed low morbidity and reduced viral copy number which was restricted to fewer tissues. The pattern suggests, biologically, that once viral replication exceeds a critical level, host control is ineffective, whereas below the threshold, individual host factors, such as genetic background, innate immune capacity, or physiological condition, may strongly influence infection trajectory (Purcell et al., 2010; Rebl and Goldammer, 2018). In the current study, fish exhibited divergent disease phenotypes at lower challenge doses (4.6×10^4 and 4.6×10^3 copies/mL), with 48.7% of fish expressing clinical disease, while 51.3% remained subclinical. Accordingly, the phenotypic variation observed among individuals at lower challenge doses may reflect genetic factors underlying disease resistance, which become more apparent when host defence mechanisms are not overwhelmed by rapid viral replication (Anacleto et al., 2019). Investigation into potential genetic factors in the current data set is on-going. The potential to select individuals with genetically mediated control that exhibit subclinical infections with low viral doses highlight the need for diagnostic approaches capable of reliably detecting infection across a wide range of viral burdens, preferably without killing fish that exhibit resistance.

4.5. Implications for RGNNV surveillance and disease management

The current study demonstrates that non-destructive samples can support RGNNV surveillance in giant grouper. As expected from the strong neurotropism of nodavirus, destructive sampling of brain and eye remains the most sensitive diagnostic approach. Urine had no diagnostic value; however, mucous exhibited high diagnostic utility, detecting RGNNV in all clinically affected fish and aligning well with neural tissues in subclinical individuals. The results of non-destructive samples demonstrated eRNA monitoring provides complementary information by capturing tank-level RGNNV detection, although the delayed detection relative to clinical signs suggests eRNA is best used to confirm ongoing infection rather than to provide early warning. Finally, combining mucous-based sampling with eRNA water surveillance can expand non-destructive diagnostic capacity for RGNNV, allowing practical monitoring of RGNNV in field-based approaches to increase the understanding of factors that lead to natural disease outbreaks.

CRediT authorship contribution statement

Ngoc-Tran T. Nguyen: Writing – original draft, Visualization, Methodology, Investigation, Formal analysis, Data curation, Conceptualization. **Junya Minami:** Writing – review & editing, Methodology, Investigation, Conceptualization. **Maria Andrade Martinez:** Writing – review & editing, Methodology, Conceptualization. **Richard M. Knuckey:** Writing – review & editing, Methodology. **Kyall R. Zenger:** Writing – review & editing, Supervision, Methodology,

Conceptualization. **Dean R. Jerry:** Writing – review & editing, Methodology, Funding acquisition, Conceptualization. **Kelly Condon:** Writing – review & editing, Supervision, Methodology, Data curation, Conceptualization.

Ethics statement

All experimental procedures involving animals were conducted in accordance with the guidelines for the care and use of animals for scientific purposes and were approved by the James Cook University Animal Ethics Committee (Approval No. A2825).

Declaration of competing interest

The authors declare that they have no known competing financial interests or personal relationships that could have appeared to influence the work reported in this paper.

Acknowledgement

This work was supported by the Australian Research Council Industrial Transformation Research Hub for Supercharging Tropical Aquaculture through Genetics (IH130200013). Staff from The Company One are gratefully acknowledged for providing the experimental animals. Staff from the James Cook University Marine Aquaculture Research Facilities Unit are thanked for their technical support in maintaining the experimental fish under quarantine conditions prior to the experiment.

Appendix A. Supplementary data

Supplementary data to this article can be found online at https://doi.org/10.1016/j.aquaculture.2026.744129.

Data availability

Data will be made available on request.

References

Aamelfot, M., McBeath, A., Christiansen, D.H., Matejusova, I., Falk, K., 2015. Infectious salmon anaemia virus (ISAV) mucosal infection in Atlantic salmon. Vet. Res. 46, 120. https://doi.org/10.1186/s13567-015-0265-1.

Alizon, S., Hurford, A., Mideo, N., Van Baalen, M., 2009. Virulence evolution and the trade-off hypothesis: history, current state of affairs and the future. J. Evol. Biol. 22, 245–259. https://doi.org/10.1111/j.1420-9101.2008.01658.x.

Anacleto, O., Cabaleiro, S., Villanueva, B., Saura, M., Houston, R.D., Woolliams, J.A., Doeschl-Wilson, A.B., 2019. Genetic differences in host infectivity affect disease spread and survival in epidemics. Sci. Rep. 9. https://doi.org/10.1038/s41598-019-40567-w.

Avunje, S., Kim, W.S., Park, C.S., Oh, M.J., Jung, S.J., 2011. Toll-like receptors and interferon associated immune factors in viral haemorrhagic septicaemia virus-infected olive flounder (*Paralichthys olivaceus*). Fish Shellfish Immunol. 31, 407–414. https://doi.org/10.1016/j.fsi.2011.06.009.

Bandín, I., Souto, S., 2020. Betanodavirus and VER disease: a 30-year research review. Pathogens 9, 106. https://doi.org/10.3390/pathogens9020106.

Bass, D., Christison, K.W., Stentiford, G.D., Cook, L.S.J., Hartikainen, H., 2023. Environmental DNA/RNA for pathogen and parasite detection, surveillance, and ecology. Trends Parasitol. 39, 285–304. https://doi.org/10.1016/j.pt.2022.12.010.

Bergelson, J.M., 2003. Virus interactions with mucosal surfaces: alternative receptors, alternative pathways. Curr. Opin. Microbiol. 6, 386–391. https://doi.org/10.1016/S1369-5274(03)00097-3.

Breuil, G., Bonami, J.R., Pepin, J.F., Pichot, Y., 1991. Viral infection (picorna-like virus) associated with mass mortalities in hatchery-reared sea-bass (*Dicentrarchus labrax*) larvae and juveniles. Aquaculture 97, 109–116. https://doi.org/10.1016/0044-8486(91)90258-9.

Brugere, C., Onuigbo, D.M., Morgan, K.L., 2017. People matter in animal disease surveillance: challenges and opportunities for the aquaculture sector. Aquaculture 467, 158–169. https://doi.org/10.1016/j.aquaculture.2016.04.012.

Butler, G., Candebat, C.L., Das, S.K., Nankervis, L., 2025. Dietary methionine and choline mediate mobilisation of plasma lipids to improve feed efficiency for the diets of giant grouper (*Epinephelus lanceolatus*). Anim. Feed Sci. Technol. 324, 116317. https://doi.org/10.1016/j.anifeedsci.2025.116317.

Chen, Y.M., Wang, T.Y., Chen, T.Y., 2014. Immunity to betanodavirus infections of marine fish. Dev. Comp. Immunol. 43, 174–183. https://doi.org/10.1016/j.dci.2013.07.019.

Condon, K., 2019. Management of Betanodavirus Infection in Queensland Giant Grouper, *Epinephelus lanceolatus* (Bloch) PhD Thesis, James Cook University. https://doi.org/10.25903/er4h-mh91.

Costa, J.Z., Thompson, K.D., 2016. Understanding the interaction between Betanodavirus and its host for the development of prophylactic measures for viral encephalopathy and retinopathy. Fish Shellfish Immunol. 53, 35–49. https://doi.org/10.1016/j.fsi.2016.03.033.

Coyle, S.D., Durborow, R.W., Tidwell, J.H., 2004. Anesthetics in Aquaculture. South. Reg. Aquac. Cent. No. 3900.

Dalla Valle, L., Zanella, L., Patarnello, P., Paolucci, L., Belvedere, P., Colombo, L., 2000. Development of a sensitive diagnostic assay for fish nervous necrosis virus based on RT-PCR plus nested PCR. J. Fish Dis. 23, 321–327. https://doi.org/10.1046/j.1365-2761.2000.00255.x.

Duan, X.Z., Liang, K., Yang, M., Zhang, M., Zuo, X., Jia, X., Li, Z., Yu, J., Luo, L., Shan, J., Zhao, H., Zhang, Y., Qin, Q., Wang, Q., 2024. Genome-wide association study identifies candidate SNPs and genes associated with red-spotted grouper nervous necrosis virus infection of the giant grouper (*Epinephelus lanceolatus*). Aquaculture 578, 740126. https://doi.org/10.1016/j.aquaculture.2023.740126.

FAO, 2025. Fishery and aquaculture statistics. Global aquaculture production 1950-2023 (FishStatJ). In: FAO Fish. Aquac. Div.. www.fao.org/fishery/en/statistics/software/fishstatj.

Farrell, J.A., Whitmore, L., Duffy, D.J., 2021. The promise and pitfalls of environmental DNA and RNA approaches for the monitoring of human and animal pathogens from aquatic sources. Bioscience 71, 609–625. https://doi.org/10.1093/biosci/biab027.

Ferreira, I.A., Costa, J.Z., Macchia, V., Dawn Thompson, K., Baptista, T., 2019. Detection of Betanodavirus in experimentally infected European seabass (*Dicentrarchus labrax*, Linnaeus 1758) using non-lethal sampling methods. J. Fish Dis. 42, 1097–1105. https://doi.org/10.1111/jfd.13015.

Frerichs, G.N., Tweedie, A., Starkey, W.G., Richards, R.H., 2000. Temperature, pH and electrolyte sensitivity, and heat, UV and disinfectant inactivation of sea bass (*Dicentrarchus labrax*) neuropathy nodavirus. Aquaculture 185, 13–24. https://doi.org/10.1016/S0044-8486(99)00337-3.

Glamuzina, B., Rimmer, M.A., 2022. Grouper aquaculture world status and perspectives. In: Biology and ecology of Groupers, pp. 166–190. https://doi.org/10.1201/b20814-9.

Graham, D.A., Brown, A., Savage, P., Frost, P., 2012. Detection of salmon pancreas disease virus in the faeces and mucus of Atlantic salmon, *Salmo salar* L., by real-time RT-PCR and cell culture following experimental challenge. J. Fish Dis. 35, 949–951. https://doi.org/10.1111/j.1365-2761.2012.01427.x.

Griffiths, S., Melville, K., 2000. Non-lethal detection of ISAV in Atlantic salmon by RT-PCR using serum and mucus samples. Bull. Eur. Assoc. Fish Pathol. 20, 157–162.

Grotmol, S., Bergh, Ø., Totland, G.K., 1999. Transmission of viral encephalopathy and retinopathy (VER) to yolk-sac larvae of the Atlantic halibut *Hippoglossus hippoglossus*: occurrence of nodavirus in various organs and a possible route of infection. Dis. Aquat. Org. 36, 95–106. https://doi.org/10.3354/dao036095.

Grove, S., Johansen, R., Dannevig, B.H., Reitan, L.J., Ranheim, T., 2003. Experimental infection of Atlantic halibut *Hippoglossus hippoglossus* with nodavirus: tissue distribution and immune response. Dis. Aquat. Org. 53, 211–221. https://doi.org/10.3354/dao053211.

Grove, S., Johansen, R., Reitan, L.J., Press, C.M.L., Dannevig, B.H., 2006. Quantitative investigation of antigen and immune response in nervous and lymphoid tissues of Atlantic halibut (*Hippoglossus hippoglossus*) challenged with nodavirus. Fish Shellfish Immunol. 21, 525–539. https://doi.org/10.1016/j.fsi.2006.03.001.

Guo, C.J., He, J., He, J.G., 2019. The immune evasion strategies of fish viruses. Fish Shellfish Immunol. 86, 772–784. https://doi.org/10.1016/j.fsi.2018.12.013.

Harikrishnan, R., Balasundaram, C., Heo, M.S., 2010. Molecular studies, disease status and prophylactic measures in grouper aquaculture: economic importance, diseases and immunology. Aquaculture 309, 1–14. https://doi.org/10.1016/j.aquaculture.2010.09.011.

Hick, P., Whittington, R.J., 2010. Optimisation and validation of a real-time reverse transcriptase-polymerase chain reaction assay for detection of betanodavirus. J. Virol. Methods 163, 368–377. https://doi.org/10.1016/j.jviromet.2009.10.027.

Ip, Y.C.A., Chen, J., Tan, L.Y., Lau, C., Chan, Y.H., Balasubramaniam, R.S., Wong, W.Y.J., Ng, K., Tan, Z.Y.B., Fernandez, C.J., Chang, S.F., Yap, H.H., 2024. Establishing environmental DNA and RNA protocols for the simultaneous detection of fish viruses from seawater. Environ. DNA 6, e418. https://doi.org/10.1002/edn3.418.

Jaramillo, D., Fielder, S., Whittington, R.J., Hick, P., 2019. Host, agent and environment interactions affecting nervous necrosis virus infection in Australian bass *Macquaria novemaculeata*. J. Fish Dis. 42, 167–180. https://doi.org/10.1111/jfd.12913.

Johannes, R.E., 2001. A possible new candidate for grouper aquaculture. SPC Live Reef Fish Inf. Bull. 31–32.

Kang, H.Y., Lee, Y., Park, J., Lee, J.Y., Heo, Y.U., Kim, N., Kim, J.O., Kwon, M.G., Park, C. Il, Kim, D.H., 2025. Environmental RNA-dased surveillance of viral hemorrhagic septicemia virus (VHSV) in olive flounder (*Paralichthys olivaceus*) aquaculture: detection dynamics and risk assessment. Environ. DNA 7, e70083. https://doi.org/10.1002/edn3.70083.

Kawato, Y., Mekata, T., Inada, M., Ito, T., 2021. Application of environmental DNA for monitoring Red Sea bream Iridovirus at a fish farm. Microbiol. Spectrum 9. https://doi.org/10.1128/spectrum.00796-21 e00796–21.

Kim, Jae Ok, Kim, S.J., Kim, Jong Oh., Kim, W.S., Oh, M.J., 2018. Distribution of nervous necrosis virus (NNV) in infected sevenband grouper, *Hyporthodus septemfasciatus* by intramuscular injection or immersion challenge. Aquaculture 489, 1–8. https://doi.org/10.1016/j.aquaculture.2018.01.042.

Kim, S.J., Kim, W.S., Oh, M.J., 2019. Differences of viral hemorrhagic septicemia virus loads among organs of dead and surviving olive flounder infected by intramuscular injection and immersion challenge. J. Aquat. Anim. Health 31, 193–200. https://doi.org/10.1002/aah.10068.

Korsnes, K., Karlsbakk, E., Devold, M., Nerland, A.H., Nylund, A., 2009. Tissue tropism of nervous necrosis virus (NNV) in Atlantic cod, gadus morhua L., after intraperitoneal challenge with a virus isolate from diseased Atlantic halibut, *Hippoglossus hippoglossus* (L.). J. Fish Dis. 32, 655–665. https://doi.org/10.1111/j.1365-2761.2009.01035.x.

Krishnan, R., Qadiri, S.S.N., Oh, M.J., 2019. Functional characterization of seven-band grouper immunoglobulin like cell adhesion molecule, Nectin4 as a cellular receptor for nervous necrosis virus. Fish Shellfish Immunol. 93, 720–725. https://doi.org/10.1016/j.fsi.2019.08.019.

Krishnan, R., Qadiri, S.S.N., Kim, J.O., Oh, M.J., 2021. Infection dynamics and shedding kinetics of nervous necrosis virus in juvenile seven band grouper using an intraperitoneal infection-cohabitation model. Aquaculture 530, 735957. https://doi.org/10.1016/j.aquaculture.2020.735957.

Lancaster, K.Z., Pfeiffer, J.K., 2012. Viral population dynamics and virulence thresholds. Curr. Opin. Microbiol. 15, 525–530. https://doi.org/10.1016/j.mib.2012.05.007.

Lapatra, S.E., Rohovec, J.S., Fryer, J.L., 1989. Detection of infectious hematopoietic necrosis virus in fish mucus. Fish Pathol. 24, 197–202. https://doi.org/10.3147/jsfp.24.197.

Liamnimitr, P., Thammatorn, W., U-thoomporn, S., Tattiyapong, P., Surachetpong, W., 2018. Non-lethal sampling for Tilapia Lake virus detection by RT-qPCR and cell culture. Aquaculture 486, 75–80. https://doi.org/10.1016/j.aquaculture.2017.12.015.

Lin, C.S., Lu, M.W., Tang, L., Liu, W., Chao, C. Ben, Lin, C.J., Krishna, N.K., Johnson, J.E., Schneemann, A., 2001. Characterization of virus-like particles assembled in a recombinant baculovirus system expressing the capsid protein of a fish nodavirus. Virology 290, 50–58. https://doi.org/10.1006/viro.2001.1157.

Mazelet, L., Dietrich, J., Rolland, J.L., 2011. New RT-qPCR assay for viral nervous necrosis virus detection in sea bass, *Dicentrarchus labrax* (L.): application and limits for hatcheries sanitary control. Fish Shellfish Immunol. 30, 27–32. https://doi.org/10.1016/j.fsi.2010.08.015.

Moody, N.J.G., Crane, M.S.J., 2014. Betanodavirus Infections of Finfish. In: Australia and New Zealand Standard Diagnostic Procedure.

Mori, K.I., Nakai, T., Muroga, K., Arimoto, M., Mushiake, K., Furusawa, I., 1992. Properties of a new virus belonging to nodaviridae found in larval striped jack (*Pseudocaranx dentex*) with nervous necrosis. Virology 187, 368–371. https://doi.org/10.1016/0042-6822(92)90329-N.

Munday, B.L., Kwang, J., Moody, N., 2002. Betanodavirus infections of teleost fish: a review. J. Fish Dis. 25, 127–142. https://doi.org/10.1046/j.1365-2761.2002.00350.x.

Olsvik, P.A., Lie, K.K., Jordal, A.E.O., Nilsen, T.O., Hordvik, I., 2005. Evaluation of potential reference genes in real-time RT-PCR studies of Atlantic salmon. BMC Mol. Biol. 6. https://doi.org/10.1186/1471-2199-6-21.

Ortega-Villaizan, M. del M., Chico, V., Perez, L., 2022. Fish innate immune response to viral infection—an overview of five major antiviral genes. Viruses 14, 1546. https://doi.org/10.3390/v14071546.

Padrós, F., Caggiano, M., Toffan, A., Constenla, M., Zarza, C., Ciulli, S., 2022. Integrated management strategies for viral nervous necrosis (VNN) disease control in marine fish farming in the Mediterranean. Pathogens 11, 1–27. https://doi.org/10.3390/pathogens11030330.

Poisa-Beiro, L., Dios, S., Montes, A., Aranguren, R., Figueras, A., Novoa, B., 2008. Nodavirus increases the expression of mx and inflammatory cytokines in fish brain. Mol. Immunol. 45, 218–225. https://doi.org/10.1016/j.molimm.2007.04.016.

Purcell, M.K., LaPatra, S.E., Woodson, J.C., Kurath, G., Winton, J.R., 2010. Early viral replication and induced or constitutive immunity in rainbow trout families with differential resistance to infectious hematopoietic necrosis virus (IHNV). Fish Shellfish Immunol. 28, 98–105. https://doi.org/10.1016/j.fsi.2009.10.005.

R Core Team, 2025. R: A Language and Environment for Statistical Computing.

Rebl, A., Goldammer, T., 2018. Under control: the innate immunity of fish from the inhibitors' perspective. Fish Shellfish Immunol. https://doi.org/10.1016/j.fsi.2018.04.016.

Rimmer, M.A., Glamuzina, B., 2019. A review of grouper (family Serranidae: subfamily Epinephelinae) aquaculture from a sustainability science perspective. Rev. Aquac. 11, 58–87. https://doi.org/10.1111/raq.12226.

Tanaka, S., Aoki, H., Nakai, T., 1998. Pathogenicity of the nodavirus detected from diseased sevenband grouper *Epinephelus septemfasciatus*. Fish Pathol. 33, 31–36. https://doi.org/10.3147/jsfp.33.31.

Tarrab, K., Ravid-Peretz, S., Ucko, M., 2019. Immunoserology of European seabass (*Dicentrarchus labrax*) and white grouper (*Epinephelus aeneus*) as a non-lethal diagnostic tool for viral nervous necrosis. Aquac. Int. 27, 63–77. https://doi.org/10.1007/s10499-018-0307-6.

Thwaite, R., Li, A., Kawasaki, M., Lin, C. han, Stephens, F., Cherrie, B., Knuckey, R., Landos, M., Barnes, A.C., 2022. Longitudinal field survey during deployment of an emergency autogenous vaccine against Betanodavirus in farmed giant grouper (*Epinephelus lanceolatus*): multiple factors contribute to outbreaks and survival. Aquaculture 548, 737599. https://doi.org/10.1016/j.aquaculture.2021.737599.

Toubanaki, D.K., Efstathiou, A., Karagouni, E., 2022. Transcriptomic analysis of fish hosts responses to nervous necrosis virus. Pathogens 11, 201. https://doi.org/10.3390/pathogens11020201.

Wargo, A.R., Scott, R.J., Kerr, B., Kurath, G., 2017. Replication and shedding kinetics of infectious hematopoietic necrosis virus in juvenile rainbow trout. Virus Res. 227, 200–211. https://doi.org/10.1016/j.virusres.2016.10.011.

WOAH, 2022. The Use of Environmental DNA Methods for Detection of WOAH Listed Aquatic Animal Diseases. WOAH Aquatic Animal Health Standards Commission.

Yang, Z., Yue, G.H., Wong, S.M., 2022. VNN disease and status of breeding for resistance to NNV in aquaculture. Aquac. Fish. 7, 147–157. https://doi.org/10.1016/j.aaf.2021.04.001.

Yong, C.Y., Yeap, S.K., Omar, A.R., Tan, W.S., 2017. Advances in the study of nodavirus. PeerJ 5, e3841. https://doi.org/10.7717/peerj.3841.

Zenke, K., Okinaka, Y., 2022. Multiple isoforms of HSP70 and HSP90 required for betanodavirus multiplication in medaka cells. Arch. Virol. 167, 1961–1975. https://doi.org/10.1007/s00705-022-05489-5.

Zhang, Z., Xing, J., Tang, X., Sheng, X., Chi, H., Zhan, W., 2024. Nectin1 is a pivotal host factor involved in attachment and entry of red-spotted grouper nervous necrosis virus in the early stages of the viral life cycle. J. Virol. 98. https://doi.org/10.1128/jvi.00901-24.